sustainability

MDPI

Article

Three-Dimensional Electrochemical Oxidation System with RuO_2-IrO_2/Ti as the Anode for Ammonia Wastewater Treatment

Zhengmin Huang [1,†], Li Zhao [1,†], Jingping Zhu [1,*] and Dongming He [2]

[1] School of Environment and Resources, Southwest University of Science and Technology, Mianyang 621010, China; hzm@mails.swust.edu.cn (Z.H.)
[2] Sichuan Hebang Biotechnology Co., Leshan 614000, China
* Correspondence: zjp@swust.edu.cn
† These authors contributed equally to this work.

Abstract: In this study, a three-dimensional electrochemical oxidation system was constructed to treat ammonia nitrogen wastewater generated from the tail gas absorption of a methionine producer by using a homemade MAC mixed with a GAC at a mass ratio of 1:2 as the particle electrode, with a RuO_2-IrO_2/Ti polar plate as the anode and a stainless steel plate as the cathode. The effects of current density, initial pH value of wastewater, plate spacing, NaCl concentration and particle filling amount on COD_{Cr} and NH_4^+-N removal were investigated through single-factor experiments, and the removal pathways of COD_{Cr} and NH_4^+-N under the system were initially explored via cyclic voltammetry curves, scanning electron microscopy and tertiary butanol quenching experiments. The experimental results showed that the average removal rate of COD_{Cr} was 91.03% and that of NH_4^+-N was 98.89% after electrolysis for 5 h under the conditions of a current density of 40 mA/cm^2, no pH adjustment, the spacing of the electrode plates of 8 cm, the NaCl dosing concentration of 1 g/L, and the particle filling amount of 400 g/L. Under this experimental condition, the removal of COD_{Cr} occurred mainly through the indirect oxidation of active chlorine and ·OH, and the removal of NH_4^+-N mainly through the indirect oxidation of active chlorine.

Keywords: three-dimensional electrode; ammonia wastewater; efficiency; removal pathway

check for updates

Citation: Huang, Z.; Zhao, L.; Zhu, J.; He, D. Three-Dimensional Electrochemical Oxidation System with RuO_2-IrO_2/Ti as the Anode for Ammonia Wastewater Treatment. *Sustainability* **2024**, *16*, 1838. https://doi.org/10.3390/su16051838

Academic Editor: Andrea G. Capodaglio

Received: 6 January 2024
Revised: 25 January 2024
Accepted: 8 February 2024
Published: 23 February 2024

Copyright: © 2024 by the authors. Licensee MDPI, Basel, Switzerland. This article is an open access article distributed under the terms and conditions of the Creative Commons Attribution (CC BY) license (https://creativecommons.org/licenses/by/4.0/).

1. Introduction

With the unprecedented development of the economy, population and urbanization, the discharge of high concentrations of difficult-to-degrade toxic wastewater from industrial production has also increased year by year [1], and how to deal with this kind of industrial wastewater is a very serious problem for our country and even for today's world. NH_4^+-N is one of the important indexes for characterizing the pollution status of water quality [2], which mainly comes from industrial wastewater discharges such as chemical industry, metallurgy, petroleum processing, and the decomposition of nitrogenous organic matter in domestic sewage as well as farmland drainage, etc. [3,4], and the hazards of wastewater containing a large amount of NH_4^+-N for aquatic environments, such as water bloom and stagnant water, blackened water bodies and odor, and disruption of the ecological balance of the water [5,6], have aroused global concern. Methionine is an important amino acid which is mainly used as an additive for feed, and industrial large-scale methionine production mainly adopts the Hein method [7], where raw materials include hydrocyanic acid, ammonium bicarbonate and other substances, so a large amount of ammonia nitrogen wastewater will be generated in the process of tail gas absorption.

The current treatment methods for ammonia wastewater mainly include physico-chemical and biological methods, such as blow-off, chemical precipitation, folding-point chlorination, ion exchange, electrochemical oxidation and biological nitrification denitrification [8,9]. The basic principle of electrochemical oxidation is to make pollutants undergo redox reactions by directly gaining or losing electrons on the electrodes, or relying on

the hydroxyl radicals and other active substances generated at the anode to degrade the pollutants [10,11]. Compared with other treatment methods, electrochemical oxidation is widely used to treat various types of industrial wastewater due to its advantages of simple equipment, independence from environmental conditions, and high treatment efficiency. However, the conventional two-dimensional electrode system has a small specific surface area, uses a large amount of electrical energy, and has a high mass transfer resistance, especially in low-conductivity wastewater, which cannot be ignored [12]. According to previous studies, this problem can be solved by placing conductive particles that will be polarized between the anode and cathode because a large number of microcells are formed in the system. This particle electrode material acts as a complex electrode in the polar plate, which can increase the face-to-body ratio, adsorption strength and conduction strength of this system. This system is usually called the three-dimensional electrode system or particle electrode system [13–15].

Common three-dimensional particle materials include metal particles, plating active material particles, activated carbon particles and so on. As conductive particles, activated carbon has become a good substitute because of its good conductivity, low cost and strong affinity. However, when putting particles in a three-dimensional electrode reactor, the current efficiency is often reduced due to the short-circuit current and bypass current of the particle electrode. Therefore, in order to improve the efficiency of the electrode reaction, it is necessary to solve this problem as far as possible. At present, particle insulation has been used to remove short-circuit currents, such as adding insulating particles in three-dimensional particle fillers. Wei [16] used granular activated carbon (GAC) and porous ceramsite (PCP) as composite particle electrodes, and a three-dimensional electrode reactor (3DER) was used to study the treatment of heavy oil refinery wastewater (HORW). The results show that compared with the two-dimensional electrode reactor (unfilled particle electrode), the chemical oxygen demand (COD) removal effect of 3DER is better, and the composite particle electrode is beneficial to improve the COD removal efficiency and reduce energy consumption. It has also been studied that the insulating material is loaded on the surface of the particles to achieve this purpose. Wang [17] and others adopt the full insulation mode of loading cellulose acetate on the particle electrode to effectively avoid the formation of a short-circuit current. In the electrocatalytic treatment of 30 min, the COD removal rate is 20% higher than that of non-insulation. It is reported [18] that the separation of particles from each other can also effectively solve this problem. The use of a particle electrode string can reduce the contact of particles and thus reduce the short-circuit current in the three-dimensional electrode system.

In order to effectively electrochemically incinerate organic molecules, the selection of anode is equally crucial. A DSA electrode is often favored because of its advantages of high catalytic activity, low tank voltage and high stability, and has been widely used in metallurgy, chlor-alkali industry and other industries [19–24]. DSA electrodes are a class of metal oxide-coated electrodes with excellent electrocatalytic activity such as Ru, Ir, Sn, etc. Ti metal is the most commonly used electrode substrate material because of its good corrosion resistance and low price. Domestic and foreign scholars have synthesized PbO_2/Ti, RuO_2-IrO_2/Ti, BDD/Ti, Sb-SnO_2/Ti and other element-doped electrodes using titanium as the electrode substrate [25–27], and the superior electrooxidative properties of BDD have been proved to be able to degrade a variety of organic molecules [28–30], but the high cost limits its large-scale application. Sb-doped SnO_2 deactivates after a few oxidation cycles, despite its low cost and excellent oxidation performance [31]. RuO_2 is considered one of the most promising anode materials due to its advantages of high specific energy, low internal resistance, wide electrochemical window and electrocatalytic activity, while IrO_2 has better stability, and by compositing RuO_2 with IrO_2, the two can synergistically enhance the electrocatalytic activity and stability of the electrode [32]. Nowadays, RuO_2-IrO_2/Ti, an electrode plate, has been widely studied and used by scholars. For example, Lic. A et al. [33] used electrochemically generated Cl_2 to eliminate cephalosporin (86 mmol/L) in different wastewaters, e.g., deionized water, municipal wastewater and urine, using RuO_2-IrO_2/Ti

as an anode, and demonstrated that electrically generated Cl_2 actives were capable of converting antibiotics into biodegradable compounds. Ukundimana Z. et al. [34] used RuO_2-IrO_2/Ti as an anode for the treatment of waste leachate, it was found that the chloride content of the leachate promoted indirect oxidation, which greatly improved the removal efficiency of COD and TOC. Oliveira et al. [35], in treating wastewater generated from the cashew processing industry using a BDD anode and Ti/RuO_2-TiO_2 anode, showed that under the same operating conditions, the BDD had a greater efficiency of COD and TOC removal than the Ti/RuO_2-TiO_2 anode, with a greater removal rate and the latter with a higher current efficiency. Zhu et al. [36] prepared RuO_2-IrO_2/Ti electrodes for the removal of aniline from wastewater via thermal oxidation using NaCl as the electrolyte, which showed the maximum removal of TOC (63.1%), and it was not easy to passivate at a high current density.

Based on the above, in this study, a three-dimensional electrode system was constructed using composite activated carbon particles of RuO_2-IrO_2/Ti as the anode and a stainless steel plate as the cathode to treat ammonia nitrogen wastewater generated from methionine industrial production, and the effects of current density, initial pH value of wastewater, spacing of the plates, concentration of NaCl, and filling amount of the particles on the removal rate of COD_{Cr} and NH_4^+-N. In addition, the removal pathways of COD_{Cr} and NH_4^+-N in wastewater were initially investigated with a view to providing theoretical references for actual wastewater treatment, helping to improve the quality of water environments and promoting sustainable development and ecological protection.

2. Materials and Methods

2.1. Experimental Materials

Experimental reagents: sodium chloride, potassium sodium tartrate, Nessler's reagent, potassium dichromate (superior purity), silver sulfate, mercuric sulfate, granular activated carbon (GAC) and cellulose acetate-coated activated carbon (MAC, self-made). All of the above reagents are analytically pure and purchased from Chron Chemicals, Chengdu, China.

The preparation process of MAC: prepare 750 mL of an 85% acetone aqueous solution, weigh 70 g cellulose acetate (CA), slowly dissolve the CA in the acetone solution and speed up the dissolution rate via stirring ultrasound. After complete dissolution, add 500 g pretreated GAC to soak for 20 min in order to speed up the coating speed and uniformity of CA on the surface of GAC. Stirring ultrasound is carried out continuously during soaking. The fully soaked GAC is taken out on the barbed wire to filter out the solvent, and then stirred and separated continuously with a glass rod, so that the GAC did not adhere and the particles were distinct. After standing at room temperature for 2 h and vacuum-drying at 60 °C for 6 h, the MAC-loaded CA was obtained.

The experimental wastewater was taken from the ammonia nitrogen wastewater generated from the tail gas absorption of a methionine producer, with a COD_{Cr} concentration of 1200~2400 mg/L, an NH_4^+-N concentration of 250~400 mg/L, a pH of 9.44~10.26 and a Cl^- concentration of 450~570 mg/L.

2.2. Experimental Device

In this experiment, a self-made three-dimensional electrode device is used, which is composed of an electrolytic cell, cathode and anode plate, particle electrode and power supply. The electrolytic cell is made of plexiglass, with the size of 12 cm × 8 cm × 9 cm and the effective volume of 0.6 L; the cathode plate is a stainless steel plate, the anode plate is an iridium ruthenium titanium-coated (RuO_2-IrO_2/Ti) plate and the anode plate is 7.5 cm × 8.5 cm × 0.1 cm (The working area is 37.5 cm^2), and the distance between the plates can be adjusted; the particle electrode is made by mixing the MAC and GAC at the mass ratio of 1:2. The power supply adopts a DC-stabilized power supply (IPD-3303SLU, Yimei Technology Co., Shenzhen, China), with a voltage range of 0~30 V and a current range of 0~3 A. The experimental device is shown in Figure 1.

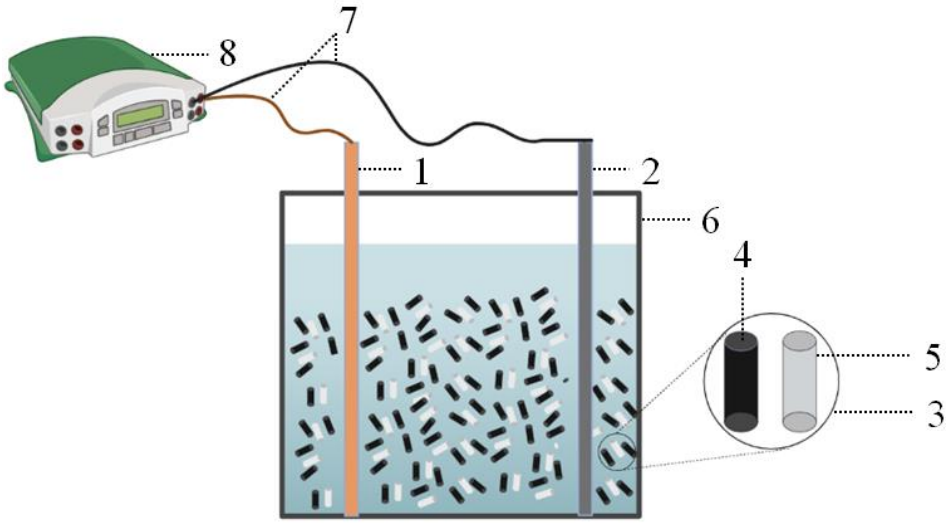

Figure 1. Schematic diagram of the experimental device (1—anode plate, 2—cathode plate, 3—particle electrode, 4—GAC, 5—MAC, 6—electrolyzer, 7—wire, 8—DC power supply).

2.3. Pretreatment of Filled Particles

In order to shield the effect of activated carbon adsorption on the treatment of ammonia nitrogen wastewater by a three-dimensional electrode, the activated carbon is washed with tap water and pure water multiple times before the use of activated carbon to remove the ash on its surface, and then baked in the oven at 105 °C for 24 h. After natural cooling, it is fully soaked in raw water, and the concentrations of COD_{Cr} and NH_4^+-N in the wastewater before and after immersion were determined. The soaking solution is then removed and the same concentration of ammonia nitrogen wastewater re-added until the concentration of COD_{Cr} and NH_4^+-N in the wastewater is basically the same before and after soaking. At this time, activated carbon reaches adsorption saturation, and the interference of activated carbon adsorption on electrolysis experiment is eliminated [37].

2.4. Experimental Design

2.4.1. Optimization of Suitable Single-Factor Conditions

Add 500 mL ammonia wastewater to the electrolytic cell, fill the particle electrode, add solid NaCl as an electrolyte, add 0.1 mol/L H_2SO_4 or 0.1 mol/L NaOH solution to adjust the pH of waste water according to the experimental requirements, turn on the power supply and start the reaction. The electrolysis time lasts 5 h, and three parallel samples are taken every 1 h to determine the concentration of COD_{Cr} and NH_4^+-N in the wastewater. Taking the removal rate of COD_{Cr} and NH_4^+-N in wastewater as the main evaluation index, the effects of single-factor conditions such as current density, initial pH value of wastewater, polar plate spacing, NaCl concentration and particle filling amount on the evaluation index are investigated, respectively, in order to select suitable single-factor conditions.

2.4.2. Explore the Removal Pathways of COD_{Cr} and NH_4^+-N

(1) Analysis of direct electrochemical oxidation involving the anode plate surface

In order to determine whether direct electrochemical oxidation exists on the surface of the RuO_2-IrO_2/Ti anode plate, the cyclic voltammetry (CV) curves of RuO_2-IrO_2/Ti before and after electrolysis are tested using a three-electrode system with an electrochemical workstation (PARSTAT4000, Princeton Company, Princeton, NJ, USA), and the positions and shapes of the peaks in the CV curves are used to analyze whether redox reactions occur on the surface of the RuO_2-IrO_2/Ti anode plate. The ruthenium–iridium–titanium (RuO_2-IrO_2/Ti) electrode was used as the working electrode, the platinum electrode as the auxiliary electrode, and the mercuric oxide (Hg/HgO/OH-) electrode as the reference electrode. The electrolyte was ammonia wastewater + 1 g/L NaCl. The scanning speed is

set at 0.1 V/s, and the cyclic voltammetry curves of the RuO_2-IrO_2/Ti electrode plate before and after the electrolysis of ammonia wastewater by the three-dimensional electrochemical oxidation system (3DEOS) are tested for a total of three laps, and the most stable lap is selected as the final curve.

Combined with a scanning electron microscope (Sigma300, Zeiss, Oberkochen, Germany) to sample the same area of the RuO_2-IrO_2/Ti anode plate before and after electrolysis, the micro-morphological changes of the RuO_2-IrO_2/Ti anode plate before and after electrolytic use are observed by varying the magnification of the SEM in order to further illustrate the existence of the surface of the RuO_2-IrO_2/Ti anode plate with direct electrochemical oxidation.

(2) Analysis of indirect electrochemical oxidation involving active chlorine

To determine the presence of indirect electrochemical oxidation by active chlorine, 500 mL of experimental wastewater is treated by electrolysis using 3DEOS under preferred single-factor conditions. The changes in COD_{Cr} and NH_4^+-N removal, total chlorine and free chlorine concentrations in the electrolysis system with electrolysis time are recorded to investigate whether active chlorine is involved in the indirect electrochemical oxidation of COD_{Cr} and NH_4^+-N in wastewater.

(3) Analysis of indirect electrochemical oxidation involving hydroxyl radicals

To determine the presence of indirect electrochemical oxidation by hydroxyl radicals (·OH), two sets of electrolytic systems were set up under the preferred one-factor conditions. The quencher of ·OH, a tertiary butyl alcohol (TBA) [38], is added to one group of electrolytic systems and not to the other group. The removal effects of COD_{Cr} and NH_4^+-N in wastewater by the two sets of electrolysis systems before and after TBA addition were compared so as to investigate whether ·OH was involved in the indirect electrochemical oxidation of COD_{Cr} and NH_4^+-N in wastewater.

2.5. Analytical Items and Measurement Methods

COD_{Cr}, NH_4^+-N and active chlorine were determined using double-beam UV–vis spectrophotometer (TU-1950) according to Chinese national standard methods HJ/T399-2007, HJ 535-2009 and HJ 586-2010, respectively. The removal efficiency of pollutants (COD_{Cr}, NH_4^+-N) at time "t" can be calculated according to the following Equation (1):

$$\text{Removal efficiency}(\%) = (C_0 - C_t)/C_0 \quad (1)$$

where C_0 is the initial concentration of pollutants (COD_{Cr}, NH_4^+-N) (mg/L), and C_t is the concentration of pollutants (COD_{Cr}, NH_4^+-N) at time "t" (mg/L).

3. Results and Discussion

3.1. Optimization of Suitable Single-Factor Conditions

3.1.1. Preferred Current Density

The experimental conditions are as follows: the concentration of electrolyte NaCl is 2 g/L, the filling amount of activated carbon is 100 g/L, the distance between plates is 6 cm, and the initial pH value of wastewater is not adjusted. With the conditions of different current densities, at 20 mA/cm^2, 30 mA/cm^2, 40 mA/cm^2, 50 mA/cm^2 and 60 mA/cm^2, the removal rates of COD_{Cr} and NH_4^+-N in the wastewater during a 5 h electrolysis period are shown in Figures 2a and 3a.

From Figure 2a, it can be seen that under the condition of the same current density, the removal rate of COD_{Cr} in wastewater increases with the increase in electrolysis time, and the removal rate of COD_{Cr} in wastewater is different with different current densities at the same time. Within 4 h before electrolysis, it was observed that the removal rate of COD_{Cr} in wastewater increased with the increase in current density. When the current density was 20, 30, 40, 50 and 60 mA/cm^2, the removal rate of COD_{Cr} reached 48.56%, 73.33%, 76.67%, 77.56% and 84.44%, respectively. This may be due to the fact that as the current density

increases, the cell voltage of the electrolytic cell increases, and the potential difference between the main electrode and the particle electrode and the electrolyte increases, resulting in the repolarization of the particle electrode in the reactor [39], the formation of more small microcells and the rapid increase in the degradation rate of COD_{Cr}. At the same time, the higher voltage enhanced the electrochemical oxidation, increased the ability of the anode to directly oxidize pollutants and promoted the degradation of COD_{Cr}. When the electrolysis continued to 4~5 h, the change range of the removal rate under different current densities was slightly smaller, which can be regarded as a stable state.

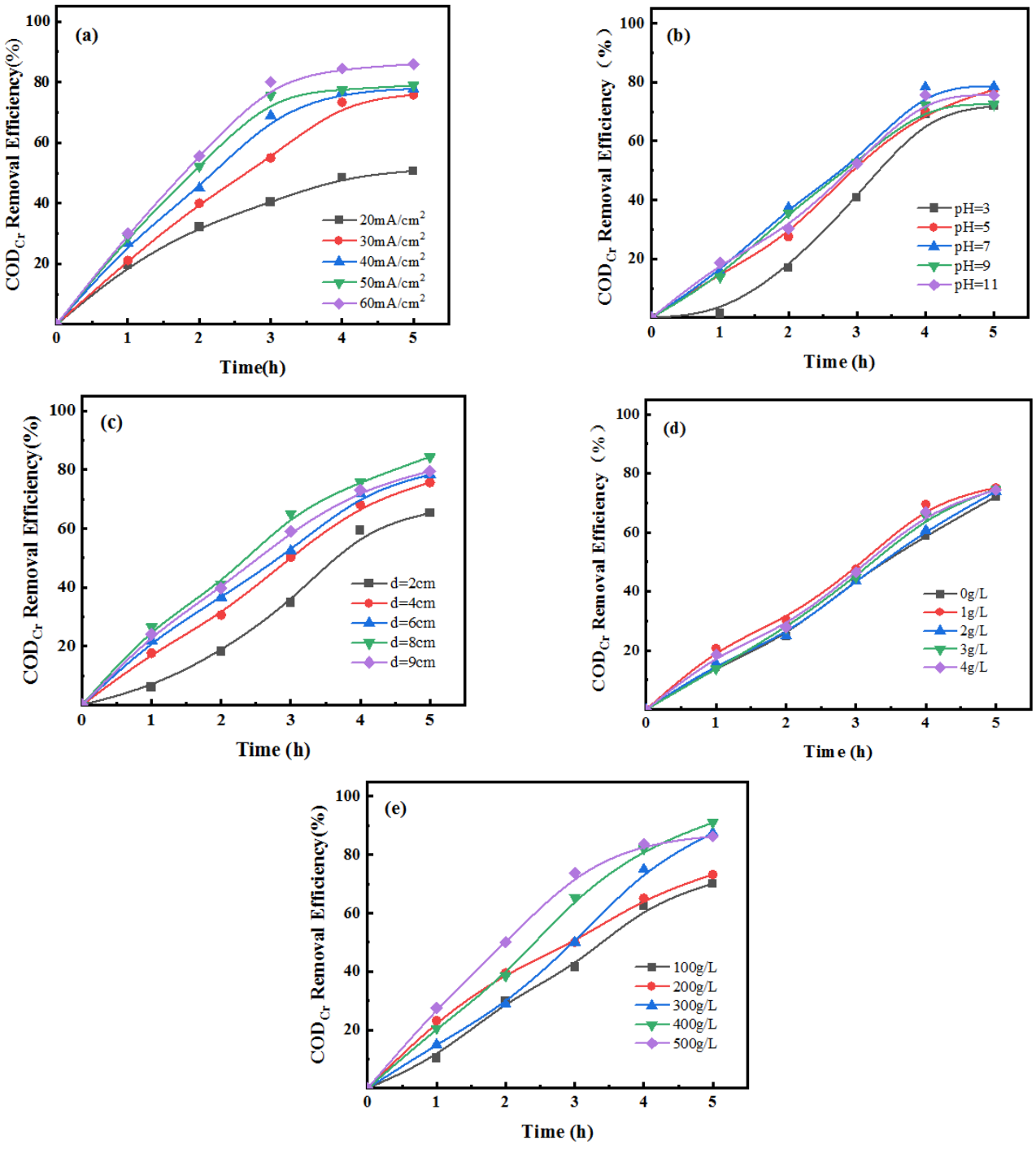

Figure 2. Effect of different single-factor condition changes on COD_{Cr} removal rate ((**a**) current density; (**b**) pH; (**c**) plate spacing; (**d**) concentration of NaCl; (**e**) particle filling amount).

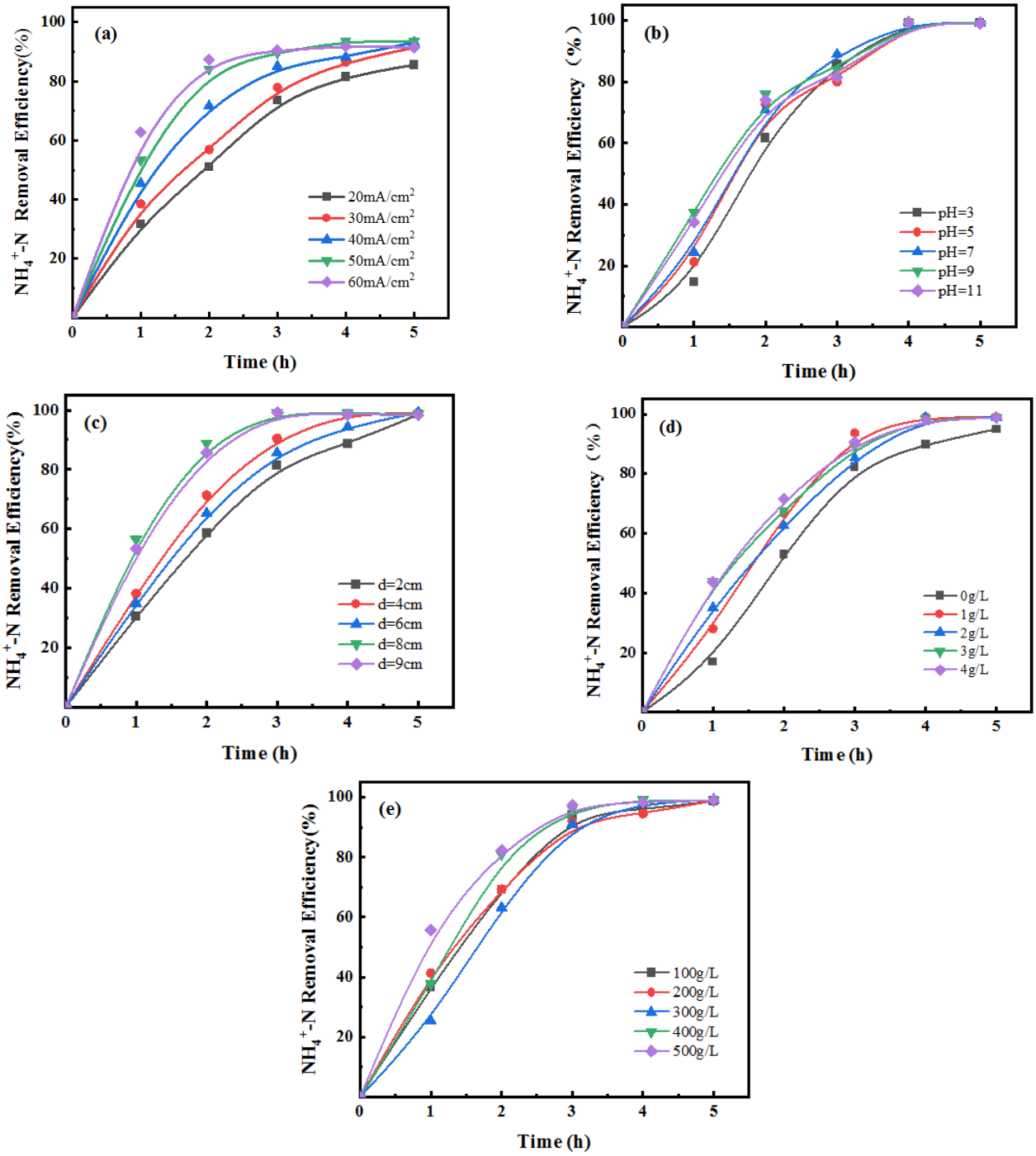

Figure 3. Effect of different single-factor condition changes on NH_4^+-N removal rate ((**a**) current density; (**b**) pH; (**c**) plate spacing; (**d**) concentration of NaCl; (**e**) particle filling amount).

As shown in Figure 3a, when the current density increases from 20 mA/cm^2 to 50 mA/cm^2, the removal rate of NH_4^+-N increases significantly, but when the current density further increases to 60 mA/cm^2, the removal rate of NH_4^+-N decreases slightly. This is due to the fact that increasing the current density within a certain range intensifies the electrochemical oxidation process and produces an increase in the concentration of active chlorine [40], which promotes NH_4^+-N removal. But when the current density exceeds a

certain degree, the cell voltage is higher than the hydrogen evolution potential of the cell reaction [41], which will aggravate the side reaction of the electrolysis system (Equation (2)).

$$4OH^- \rightarrow O_2 + 2H_2O + 4e^- \quad (2)$$

In the process of electrolysis, it can be observed that a large number of bubbles are absorbed on the electrode plate, which not only hinder the formation of holes and ·OH [42] on the surface of the anode plate, weaken the indirect oxidation ability of the 3DEOS, but also hinder the direct contact between the pollutant and the electrode plate, thus limiting the reaction efficiency of the electrochemical oxidation of the three-dimensional electrode.

To sum up, with the increase in current density within a certain range, the removal rates of COD_{Cr} and NH_4^+-N increase, considering that the increase in current density will aggravate the plate corrosion and the energy consumption will increase accordingly. Therefore, considering the removal rate of NH_4^+-N and COD_{Cr}, current efficiency and power consumption and other factors, the current density selected in this experiment is 40 mA/cm^2.

3.1.2. Preferred Initial pH of Wastewater

The experimental conditions are as follows: the current density is 40 mA/cm^2, the concentration of electrolyte NaCl is 2 g/L, the filling amount of activated carbon is 100 g/L and the distance between plates is 6 cm. With pH = 3, pH = 5, pH = 7, pH = 9 and pH = 11 being used, the removal rates of COD_{Cr} and NH_4^+-N in the wastewater during the 5 h electrolysis period are shown in Figures 2b and 3b.

The experimental results show that under different pH conditions, the removal rate of COD_{Cr} in each 3DEOS increases with the increase in electrolysis time, and until 4 h after electrolysis, the removal rate of COD_{Cr} in each 3DEOS tends to be stable. In the process of electrolysis in the first 4 h, only when pH = 3 was used, the removal rate of COD_{Cr} in the 3DEOS was obviously lower than that in the case of pH = 5~11, and the removal rate of COD_{Cr} in the electrolysis system changed slightly when the pH increased from 5 to 11, and the effect of the initial pH value on COD_{Cr} removal was pH = 7 > pH = 11 > pH = 9 > pH = 5 > pH = 3. When the electrolysis continued to the fifth hour, the removal rate of COD_{Cr} by the 3DEOS under different initial pH values was 71.83% and 77.5%, and there was no significant difference. According to the analysis of reference [43], in the 3DEOS, when H_2O discharges at the metal oxide anode (marked as MO_x) to produce the active substance ·OH to degrade or remove the COD_{Cr} of the wastewater, the following reactions (Equations (3) and (4)) may occur:

$$MO_x + 2H_2O \rightarrow MO_x(\cdot OH) + H^+ + e^- \quad (3)$$

$$\mathrm{R} + 2\cdot OH \rightarrow RO + H_2O \quad (4)$$

In a strong acidic environment, the high concentration of H^+ causes the reaction represented by Equation (3) to shift to the left, which will affect the formation of ·OH in the anodic discharge of H_2O, which makes the degradation effect of COD_{Cr} worse.

As can be seen from Figure 3b, there is no significant difference in the removal efficiency of NH_4^+-N by 3DEOS under different initial pH values. In the first 2 h of electrolysis, the treatment effect of a pH = 7~11 system on NH_4^+-N is better than that of a pH = 3~5 system on NH_4^+-N removal. The effect of an initial pH value on NH_4^+-N removal is pH = 9 > pH = 11 > pH = 7 > pH = 5 > pH = 3. The chemical reactions that may occur in the electrolytic system are as follows:

$$2Cl^- \rightarrow Cl_2 + 2e^- \quad (5)$$

$$Cl_2 + H_2O \rightarrow HClO + HClO \quad (6)$$

$$2NH_4^+ + 6\cdot OH \rightarrow N_2\uparrow + 6H_2O + 2H^+ \quad (7)$$

$$2NH_4^+ + 3HClO \rightarrow N_2\uparrow + 3H_2O + 5H^+ + 3Cl^- \quad (8)$$

$$NH_4^+ + OH^- \rightarrow NH_3\uparrow + H_2O \quad (9)$$

$$2HClO + ClO^- + 2OH^- \rightarrow ClO_3^- + 2Cl^- + 2H_2O \quad (10)$$

When the pH value of the solution is low, the reaction represented by Equation (6) shifts to the left, and the chlorine produced via electrolysis easily escapes, so that the content of oxidizing hypochlorite is reduced. At this time, the ·OH produced by the electrode is mainly used to oxidize NH_4^+-N (Equation (7)), and its oxidation capacity is limited. With the progress of electrolysis, the pH value of wastewater increases gradually. Under neutral conditions, the solubility of chlorine produced by the anode increases, the concentration of HClO or ClO^- increases, and the synergistic effect with ·OH produced via electrolysis accelerates the oxidation of NH_4^+-N (Equation (8)). In addition, with the increase in pH in the wastewater from the electrochemical process, some NH_4^+-N will also be transformed into NH_3 (Equation (9)), but when the initial pH value of the solution is too large, HClO and ClO^- will react (Equation (10)), resulting in the decrease in active chlorine and the weakening of NH_4^+-N removal efficiency. With the continuation of electrolysis, the pH values of solutions in different systems are getting closer and closer, and there is no significant difference in the removal rate of NH_4^+-N in each 3DEOS. At the fourth hour of electrolysis, the NH_4^+-N in the system with different initial pH values is basically removed; at the fifth hour of electrolysis, all 3DEOSs reach electrolysis saturation.

To sum up, the change in the initial pH value of the wastewater under the electrolysis system has little effect on the removal efficiency of COD_{Cr} and NH_4^+-N. Now that the initial pH value of the original wastewater is 9.44~10.26, the removal effect of CODCr and NH_4^+-N by the 3DEOS without adjusting the initial pH value of the wastewater is not much different from that of the 3DEOS after adjusting the pH. At the same time, considering the loss of adding materials and manpower, the initial pH value of the wastewater can no longer be adjusted in the later experiment.

3.1.3. Preferred Polar Plate Spacing

The experimental conditions are as follows: the current density is 40 mA/cm^2, the initial pH value of wastewater is not adjusted, the concentration of NaCl is 2 g/L and the filling amount of activated carbon is 100 g/L. With plate spacings of 2 cm, 4 cm, 6 cm, 8 cm and 9 cm, the removal rates of COD_{Cr} and NH_4^+-N in the wastewater are shown in Figures 2c and 3c during the 5 h electrolysis period.

From Figure 2c, it can be seen that the change in plate spacing has a great influence on the removal rate of COD_{Cr} in wastewater. Under the condition of d = 2 cm, the treatment effect of 3DEOS on COD_{Cr} is significantly lower than that of 4 cm, 6 cm, 8 cm and 9 cm. This is because the distance between the plates is too small and a large number of filled particles are dissociated outside the two plates, which affects the polarization effect of activated carbon particles [44]. The working particle electrode is limited, which reduces the removal rate of pollutants and is easy to cause a plate short circuit, which is not conducive to the reaction. With the gradual increase in the distance between the plates, more filled particles are repolarized, the working particle electrode is increased and the removal rate of the pollutants is accelerated. However, when the plate spacing increases to 9 cm, the treatment effect of 3DEOS on COD_{Cr} is lower than that when the plate spacing is 8 cm. This is because when the plate spacing is increased, the mass transfer resistance in the reactor also increases; at the same time, it will lead to the increase in waste liquid temperature, and the electric energy is used for heating and side reaction to some extent [39,45,46].

From Figure 3c, it can be seen that the treatment effect of 3DEOS on NH_4^+-N is different with different plate spacings. In the first 4 h of the electrolysis process, with the increase in electrolysis time, the removal rate of NH_4^+-N in each electrolysis system increases continuously. When the electrode spacing is 2 cm, 4 cm, 6 cm, 8 cm and 9 cm, the removal rates of NH_4^+-N by the 3DEOS are 88.59%, 98.78%, 94.23%, 98.94% and 98.5%, respectively. When the electrode plate is 8 cm, the maximum removal rate of NH_4^+-N is 98.94%. When the spacing is gradually adjusted to 4 cm, the removal rate of ammonia

nitrogen reaches 98.78%. The number of microcells generated in the 3DEOS is the main factor affecting the electrolysis efficiency. When the plate spacing is small, the number of microcells generated is lower, and the treatment effect of wastewater is limited, while when the plate spacing is adjusted to 6~9 cm, although more microcells are formed in the electrolysis system, the current intensity becomes smaller, so the electrolysis efficiency is lower at d = 6 and d = 9 cm compared to d = 4 cm. When continuing electrolysis to the fifth hour, the treatment effect of 3DEOS on NH_4^+-N tends to be stable, and the removal rate of NH_4^+-N in each system is more than 98%.

Considering the mass transfer resistance and pollutant removal efficiency of the 3DEOS, the polar plate spacing is selected as 8 cm.

3.1.4. Preferred Concentration of NaCl

The experimental conditions are as follows: the current density is 40 mA/cm^2, the initial pH value of wastewater is not adjusted, the distance between plates is 8 cm, and the filling amount of activated carbon is 100 g/L. With the concentrations of NaCl at 0 g/L, 1 g/L, 2 g/L, 3 g/L and 4 g/L, respectively, the removal rates of COD_{Cr} and NH_4^+-N in the wastewater are shown in Figures 2d and 3d during the 5 h electrolysis period.

From the analysis of Figure 2d, it can be seen that the removal rate of COD_{Cr} in the 3DEOS with NaCl is higher than that in 3DEOS without NaCl. As an electrolyte, the appropriate NaCl dosage can effectively promote the removal of COD_{Cr}, but the excessive dosage will lead to a reduction in COD_{Cr} removal instead. After electrolysis for 5 h, the removal rates of NaCl in the electrolysis system with the dosage of 0 g/L, 1 g/L, 2 g/L, 3 g/L and 4 g/L were 72.12%, 75.17%, 73.81%, 74.71% and 74.42%, respectively. Cl^- introduced by NaCl as electrolyte will produce HClO and ClO_3^- in the process of electrocatalytic oxidation (Equations (11)–(13)). HClO and ClO_3^- have strong oxidizability and can gradually decompose organic macromolecules into small molecules (Equation (14)). Therefore, the treatment effect of COD_{Cr} in the electrolytic system with NaCl is better than that without the electrolyte. When excessive NaCl is added, the current in the electrolytic cell will be too large, the effective current and bypass current will increase at the same time, and the bypass current will increase much more than the effective current, thus reducing the current efficiency [47]. If the concentration of electrolyte is too high, a large amount of energy will be used in the side reaction, which will decrease the efficiency of the main reaction and lead to the deterioration of the treatment effect of wastewater [48].

$$2Cl^- - 2e^- \rightarrow Cl_2 \quad (11)$$

$$Cl_2 + H_2O \rightarrow HClO + H^+ + Cl^- \quad (12)$$

$$\mathrm{HClO} \rightarrow H^+ + ClO^- \quad (13)$$

$$\mathrm{R} + ClO^- \rightarrow RO + Cl^- \quad (14)$$

According to the analysis of Figure 3d, the addition of NaCl can obviously promote the removal of NH_4^+-N. In the electrolysis system with the addition of NaCl, Cl^- is electrochemical reacted to form active chlorine, and NH_4^+-N is similar to the "break point chlorination reaction" [49] to be removed (Equation (15) and (16)). However, adding too much NaCl will also limit the removal of NH_4^+-N.

$$2\mathrm{NH_4^+} + 3\mathrm{HClO} \rightarrow \mathrm{N_2} \uparrow + 3\mathrm{H_2O} + 5\mathrm{H^+} + 3\mathrm{Cl^-} \quad (15)$$

$$2\mathrm{NH_4^+} + 3\mathrm{ClO^-} \rightarrow \mathrm{N_2} \uparrow + 3\mathrm{H_2O} + 2\mathrm{H^+} + 3\mathrm{Cl^-} \quad (16)$$

In summary, the addition of an electrolyte can adjust the electrical conductivity of the solution, and then increase the conductivity, so an electrolyte is a dynamic factor in the electrolytic treatment of COD_{Cr} and NH_4^+-N by 3DEOS. An appropriate electrolyte concentration can improve the removal efficiency of COD_{Cr} and NH_4^+-N in wastewater, but if the concentration of NaCl is too high, it will not have a positive effect on the electrolysis

efficiency. Considering the cost of electrolyte addition, removal efficiency and the impact on the subsequent domestic treatment of wastewater, the concentration of NaCl selected in this study is 1 g/L.

3.1.5. Preferred Particle Filling Amount

The experimental conditions are as follows: the current density is 40 mA/cm^2, the initial pH value of wastewater is not adjusted, the distance between electrodes is 8 cm and the concentration of NaCl is 1 g/L. With the particle filling amounts being 100 g/L, 200g/L, 300 g/L, 400 g/L and 500 g/L, the removal rate of COD_{Cr} and NH_4^+-N in the wastewater is shown in Figures 2e and 3e.

As shown in Figure 2e, the change in particle filling amount has a significant effect on the treatment efficiency of wastewater COD_{Cr}. After electrolysis for 5 h, the removal rates of COD_{Cr} were 70.13%, 73.26%, 87.5%, 91.03% and 86.25%, respectively, when the particle filling amounts were 100 g/L, 200 g/L, 300 g/L, 400 g/L and 500 g/L. When the filling amount of the particles is low, the number of microbatteries generated in the system becomes lower and the electrical conductivity of the waste liquid is lower, so the treatment efficiency of wastewater by 3DEOS is lower. With the increase in particle dosage, more activated carbon particles in the solution are repolarized [50], which means that more small microbatteries are formed. Coupled with the strong adsorption caused by the rich pore structure of activated carbon particles, the directional transport distance of ions between electrodes is shortened, and the mass transfer effect is enhanced [51], thus improving the removal rate of COD_{Cr}. However, too much particle filling will lead to particle electrode agglomeration and deposition, affect the diffusion of pollutants on the particle electrode surface [52], slow down the mass transfer rate, increase the short-circuit current, and reduce the removal rate of COD_{Cr}.

As shown in Figure 3e, different particle filling amounts have different effects on NH_4^+-N. Under the condition of different particle filling amounts, the removal rate was faster in the first 3 h and achieved better results in the third hour. When the particle filling amounts were 100 g/L, 200 g/L, 300 g/L, 400 g/L and 500 g/L, the removal rates of NH_4^+-N were 94.13%, 91.91%, 90.97%, 96.23% and 97.39%, respectively. The removal rate of ammonia nitrogen was slowed down after continuous electrolysis, and ammonia nitrogen could be basically removed after 5 h of electrolysis. In a certain range, with the increase in the particle filling amount, the number of particle electrodes involved in induced charging in the electrolytic cell increases, providing more electrochemical reaction interfaces and reaction sites, and thus improving the removal rate of NH_4^+-N; adding excessive filled particles will increase the mass transfer resistance and short-circuit current in the system, resulting in a decline of the treatment effect of NH_4^+-N in the 3DEOS.

To sum up, the increase in particle filling in a certain range is conducive to the removal of COD_{Cr} and NH_4^+-N, but the removal efficiency of pollutants decreases beyond a certain limit, and at the same time, it will increase the energy consumption and input cost of the reactor, so the particle filling amount selected in this study is 400 g/L.

3.2. Removal Pathways of COD_{Cr} and NH_4^+-N

There are two pathways of electrochemical oxidation, i.e., direct electrochemical oxidation and indirect electrochemical oxidation. In the direct oxidation process, the organic matter adsorbed on the electrode surface is oxidized. On the other hand, the indirect oxidation process relies on electrically generated oxidants such as ·OH, active chlorine (e.g., HClO and ClO^-), etc., and occurs in solution rather than on the electrode surface [53,54]. CV tests and SEM characterization of RuO_2-IrO_2/Ti anode plates, TBA quenching experiments and the determination of active chlorine in the wastewater were performed to investigate the removal pathways of COD_{Cr} and NH_4^+-N in ammonia nitrogen wastewater under electrochemical oxidation.

3.2.1. Analysis of Direct Electrochemical Oxidation Involved in the Surface of Anode Plates

(1) Cyclic Voltammetry Curve

The cyclic voltammetry curve (CV) of a RuO_2-IrO_2/Ti plate in ammonia nitrogen wastewater is shown in Figure 4.

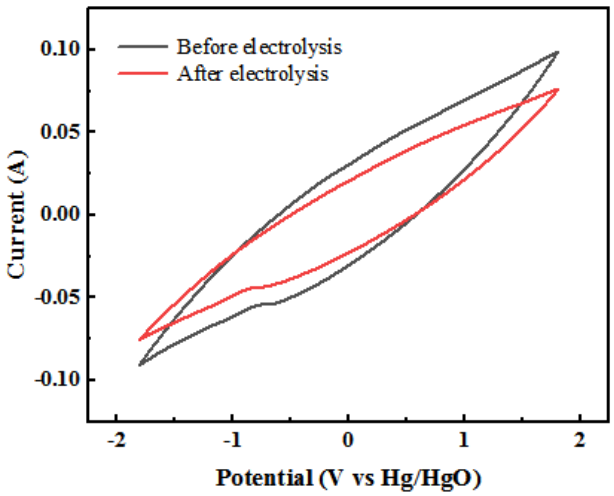

Figure 4. Cyclic voltammetry curves of RuO_2-IrO_2/Ti in ammonia nitrogen wastewater.

As shown in Figure 4, there is no characteristic peak [55] of anodic catalytic oxidation in the CV diagram of a RuO_2-IrO_2/Ti plate before and after the electrolysis of ammonia nitrogen wastewater by 3DEOS. That is, when the scanning speed is 0.1 V/s, the relationship between the current and voltage is basically linear, indicating that the target pollutants in ammonia nitrogen wastewater hardly have an electrochemical oxidation reaction directly on the surface of a RuO_2-IrO_2/Ti plate. In the 3DEOS, there is no direct electrochemical oxidation of the anode plate.

(2) Scanning Electron Microscope (SEM)

The surface morphology of a RuO_2-IrO_2/Ti plate before and after electrolysis of ammonia nitrogen wastewater can be seen via scanning electron microscope, which can be used to confirm whether the RuO_2-IrO_2/Ti plate is contaminated by ammonia nitrogen wastewater. Figure 5a,b shows the SEM characterization of a RuO_2-IrO_2/Ti plate before and after the 3DEOS of ammonia nitrogen wastewater.

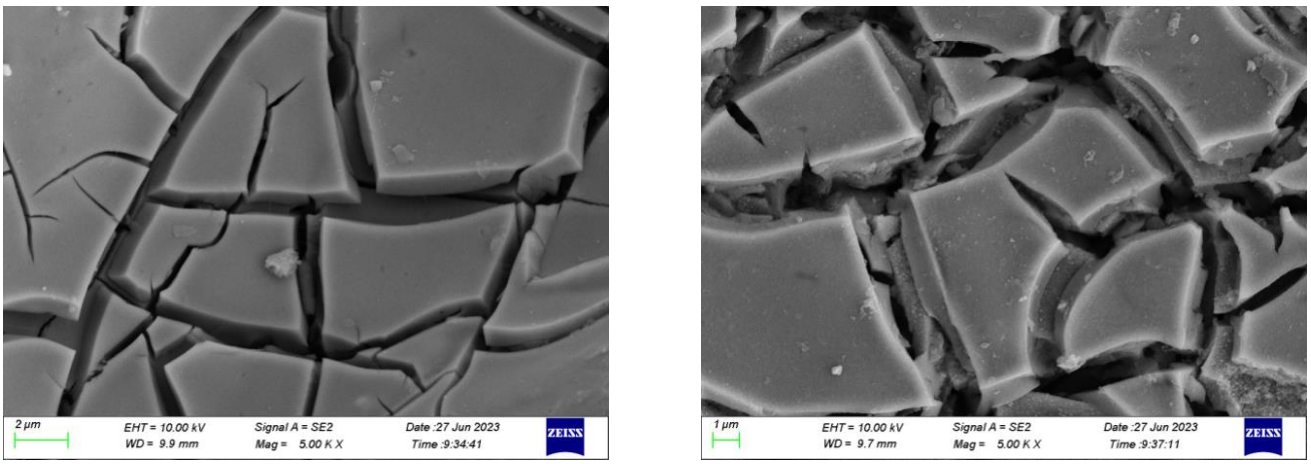

(**a**) (**b**)

Figure 5. SEM images of RuO_2-IrO_2/Ti ((**a**) before electrolysis; (**b**) after electrolysis).

As shown in Figure 5, the surface of a RuO_2-IrO_2/Ti electrode plate shows a typical mud crack morphology uniformly [56] before electrolytic treatment of ammonia nitrogen wastewater, and there is still a certain amount of gap on the surface of a RuO_2-IrO_2/Ti electrode plate. The crack is caused by the difference in the thermal expansion coefficient between the metal oxide coating loaded on the electrode plate and the titanium plate. Some cracking occurred in the metal oxide coating during the process of high-temperature roasting and subsequent cooling. After the completion of the electrolytic treatment of ammonia nitrogen wastewater, the surface structure of the RuO_2-IrO_2/Ti electrode plate is almost unchanged compared with that before the electrolytic treatment of ammonia nitrogen wastewater, and the surface of the plate only slightly dissolves. This is because the oxide layer on the surface of the plate dissolves slightly under the action of the electric field. This phenomenon shows that the RuO_2-IrO_2/Ti electrode plate is not polluted in the process of electrolytic treatment of ammonia nitrogen wastewater, and the direct electrochemical oxidation process on the electrode plate surface is not the main oxidative degradation mechanism of the target pollutants in the electrolytic treatment of ammonia nitrogen wastewater with RuO_2-IrO_2/Ti electrode plates.

From the above analysis, it can be concluded that the anode plate surface is not involved in the direct electrochemical oxidation of COD_{Cr} and NH_4^+-N in the wastewater.

3.2.2. Analysis of Indirect Electrochemical Oxidation Involving Activated Chlorine

During the 5 h electrolysis period, the changes in COD_{Cr} and NH_4^+-N removal, total chlorine and free chlorine concentrations in the electrolysis system with electrolysis time are shown in Figure 6.

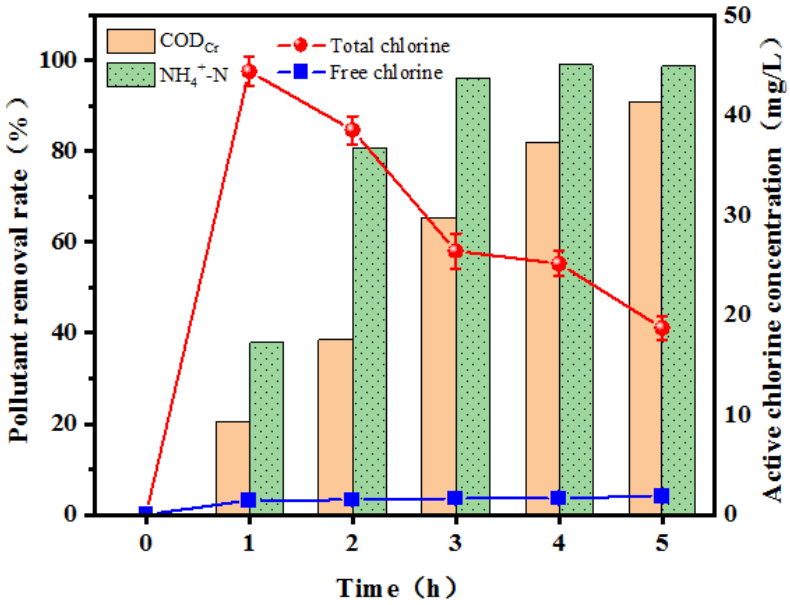

Figure 6. Removal of COD_{Cr} and NH_4^+-N in the electrolysis system and changes in total and free chlorine concentrations.

As can be seen from Figure 6, the total chlorine concentration in the wastewater shows a rapid increase and then decreasing trend: free chlorine increases to a certain concentration and then remains stable, and the COD_{Cr} and NH_4^+-N removal rate increases with the increase in electrolysis time.

After 1 h of electrolysis, the total chlorine concentration increased rapidly to 44.4 mg/L, and then decreased to 18.7 mg/L by the fifth hour. The reason for this is that during the first 1 h of electrolysis, the chlorine ions in the electrolyte continuously react with chlorine precipitation at the anode, which results in an increase in the total chlorine concentration in the solution. With the increase in electrolysis time, as the generated active chlorine

was used for the removal of pollutants (COD_{Cr} and NH_4^+-N), the active chlorine was continuously consumed, which resulted in a decrease in total chlorine concentration. The reason why the free chlorine concentration remains low is also due to the fact that the active chlorine generated during electrolysis is continuously used to react with the pollutants, and the limited amount of active chlorine generated cannot be accumulated and preserved. This result is consistent with the results reported by Wang [57], whereby the correlation between the total and active chlorine concentrations in the effluent of the secondary sedimentation tanks of a wastewater treatment plant applied to the oxidative degradation of wastewater treatment plants with the advancement of time and the degradation of the target pollutants.

In summary, activated chlorine was involved in the indirect electrochemical oxidative removal of COD_{Cr} and NH_4^+-N from the wastewater.

3.2.3. Analysis of Indirect Electrochemical Oxidation Involving ·OH

During the 5 h electrolysis period, the changes in COD_{Cr} and NH_4^+-N removal in the two electrolysis systems before and after TBA addition are shown in Figure 7.

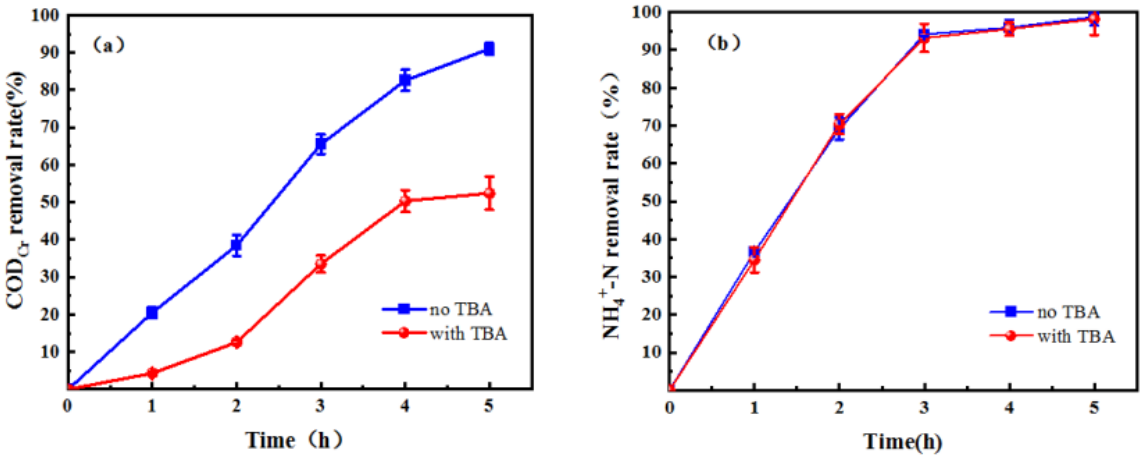

Figure 7. Removal of COD_{Cr} and NH_4^+-N by two sets of electrolysis systems ((**a**) removal of COD_{Cr}; (**b**) removal of NH_4^+-N).

As shown in Figure 7a, during the electrolysis process of 5 h, the removal rate of COD_{Cr} in wastewater by both electrolysis systems increased with the increase in electrolysis time; there was a difference in the removal rate of COD_{Cr} in wastewater by electrolysis up to the same time, and the removal rate of COD_{Cr} in wastewater by the electrolysis system with the addition of TBA was obviously lower than that by the electrolysis system without the addition of TBA. At the fifth hour of electrolysis, the removal rate of COD_{Cr} in wastewater by the electrolysis system without TBA was 91.03%, while the removal rate of COD_{Cr} in wastewater by the electrolysis system with TBA was only 52.44%. It can be seen that ·OH is involved in the oxidative removal of COD_{Cr} from wastewater during the electrolysis process of the three-dimensional electrode system.

As shown in Figure 7b, the removal rate of NH_4^+-N in wastewater by both electrolysis systems increased with the increase in electrolysis time during 5 h of electrolysis; the difference in the NH_4^+-N removal rate of wastewater by electrolysis up to the same time was very small. From electrolysis up to the first hour to electrolysis up to the fifth hour, the removal rate of NH_4^+-N in wastewater increased from 36.59% to 98.72% for the electrolysis system without TBA, and increased from 34.48% to 98.17% for the electrolysis system with TBA. It can be seen that ·OH is hardly involved in the oxidative removal of NH_4^+-N from wastewater during the electrolysis process of the 3DEOS.

Through literature [58–62] studies, as well as the test analysis of the RuO_2-IrO_2/Ti anode plates and the experimental data described above, based on the basic principle of an

electrochemical redox reaction, the migration and transformation of COD_{Cr} and NH_4^+-N in the reacting solution can be roughly understood as shown in Figure 8.

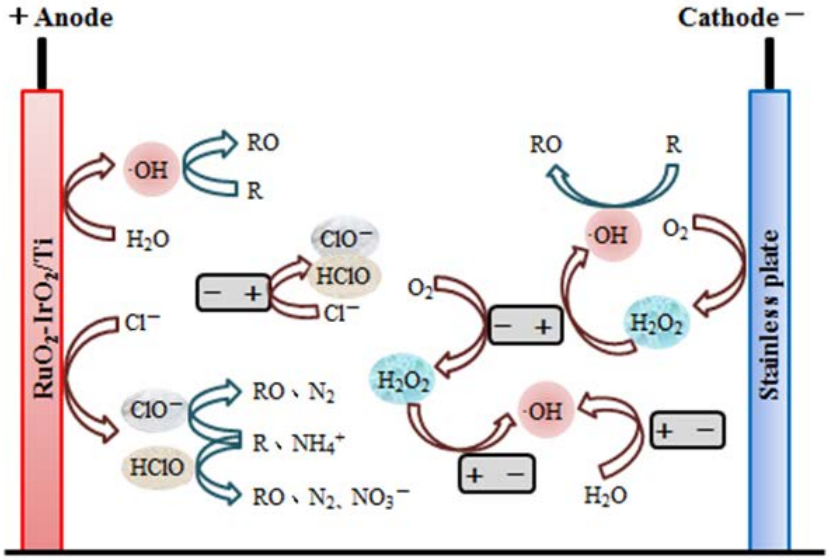

Figure 8. Electrocatalytic oxidation mechanism of 3DEOS.

The reaction process of electrocatalytic oxidation of ammonia nitrogen wastewater can be seen from the figure as shown represented by the following equations:

Main reaction equations in the anode region:

$$H_2O - e^- \rightarrow \cdot OH + H^+ \quad (17)$$

$$2Cl^- - 2e^- \rightarrow Cl_2 \quad (18)$$

Main reaction equations in the cathode region:

$$O_2 + 2e^- + 2H^+ \rightarrow H_2O_2 \quad (19)$$

Main reaction equations for solution systems:

$$Cl_2 + H_2O \rightarrow HClO + H^+ + Cl^- \quad (20)$$

$$\mathrm{HClO} \rightarrow H^+ + ClO^- \quad (21)$$

$$\mathrm{R} + 2\cdot\mathrm{OH} \rightarrow \mathrm{RO} + H_2O \quad (22)$$

$$\mathrm{R} + H_2O_2 \rightarrow \mathrm{RO} + H_2O \quad (23)$$

$$\mathrm{R} + ClO^- \rightarrow RO + Cl^- \quad (24)$$

$$\mathrm{R} + \mathrm{HClO} \rightarrow RO + H^+ + Cl^- \quad (25)$$

$$2\mathrm{NH_4}^+ + 3\mathrm{HClO} \rightarrow \mathrm{N_2} \uparrow + 3\mathrm{H_2O} + 5\mathrm{H}^+ + 3\mathrm{Cl}^- \quad (26)$$

$$2\mathrm{NH_4}^+ + 3\mathrm{ClO}^- \rightarrow \mathrm{N_2} \uparrow + 3\mathrm{H_2O} + 2\mathrm{H}^+ + 3\mathrm{Cl}^- \quad (27)$$

$$\mathrm{NH_4}^+ + 4\mathrm{HClO} \rightarrow NO_3^- + \mathrm{H_2O} + 6\mathrm{H}^+ + 4\mathrm{Cl}^- \quad (28)$$

4. Conclusions

In this study, a three-dimensional electrochemical oxidation system was constructed by mixing activated carbon loaded with cellulose acetate and activated carbon according to the mass ratio of 1:2 as a particle electrode, RuO_2-IrO_2/Ti as the anode and a stainless steel plate as the cathode for the treatment of ammonia nitrogen wastewater. According to the above research results and analysis, the following conclusions can be drawn:

(1) The suitable single-factor conditions under the 3DEOS are as follows: the current density is 40 mA/cm^2, the pH is not adjusted, the polar plate spacing is 8 cm, the NaCl concentration is 1 g/L and the particle filling amount is 400 g/L. Under these conditions, the average removal rate of COD_{Cr} and NH_4^+-N is 91.03% and 98.89%, respectively.

(2) In this study, the removal pathway of COD_{Cr} and NH_4^+-N did not include the direct electrochemical oxidation of the anode plate; in the indirect oxidation, activated chlorine was involved in the electrochemical oxidation of COD_{Cr} and NH_4^+-N in the wastewater, and ·OH was involved in the electrochemical oxidation of COD_{Cr}.

(3) An efficient and environmentally friendly ammonia nitrogen wastewater treatment method is provided, with a view to providing theoretical references for practical wastewater treatment, helping to improve the quality of the water environment and promoting sustainable development and ecological protection.

Author Contributions: Z.H.: Methodology, Software, Formal Analysis, Writing—Original Draft, Visualization; L.Z.: Conceptualization, Writing—Reviewing and Editing, Funding acquisition, Project administration; J.Z.: Review and Editing, Supervision; D.H.: Resources. All authors have read and agreed to the published version of the manuscript.

Funding: The authors acknowledge the Sichuan Provincial Science & Technology Department for financial support [grant number 2021YFG0116]. We thank the anonymous reviewers for their comments, which greatly improved the paper.

Institutional Review Board Statement: Not applicable.

Informed Consent Statement: Not applicable.

Data Availability Statement: Data will be made available on request.

Conflicts of Interest: The authors declare that they have no known competing financial interests or personal relationships that could have appeared to influence the work reported in this paper.

References

1. Yang, C.; Chen, Y.; Ouyang, K.; Yang, J.; Li, J. Current research situation and prospect of ammonia nitrogen wastewater treatment technology. *Ind. Water Treat.* **2018**, *38*, 1–5.
2. Liu, L. Research status of discharge and treatment of ammonia nitrogen wastewater in China. *Sci. Technol. Inf.* **2012**, *19*, 46.
3. Brennan, B.; Lawler, J.; Regan, F. Recovery of viable ammonia-nitrogen products from agricultural slaughterhouse wastewater by membrane contactors: A review. *Environ. Sci.-Water Res. Technol.* **2021**, *7*, 259–273. [CrossRef]
4. Scherger, L.E.; Zanello, V.; Lexow, C. Impact of Urea and Ammoniacal Nitrogen Wastewaters on Soil: Field Study in a Fertilizer Industry (Bahia Blanca, Argentina). *Bull. Environ. Contam. Toxicol.* **2021**, *107*, 565–573. [CrossRef] [PubMed]
5. Xie, J.; Liu, H.; Wang, A. Analysis of ammonia nitrogen, total nitrogen, triple nitrogen conversion and the role of ammonia nitrogen in the evaluation and control of water pollution. *Inn. Mong. Water Resour.* **2011**, 34–36.
6. Wosiack, P.A.; Lopes, D.D.; Damianovic, M.H.R.Z.; Foresti, E.; Granato, D.; Barana, A.C. Removal of COD and nitrogen from animal food plant wastewater in an intermittently-aerated structured-bed reactor. *J. Environ. Manag.* **2015**, *154*, 145–150. [CrossRef] [PubMed]
7. Gao, W.; Li, L.; Zhang, J. Advance in production process and key manufacture technology for methionine. *Chem. Ind. Eng. Prog.* **2012**, *31*, 866–872+888.
8. Wang, L.; Mou, C.; Wang, L. Treatment Methods and Research Status of High Ammonia-Nitrogen Content Wastewater. *Technol. Water Treat.* **2021**, *47*, 1–5+10.
9. Yao, Q.; Tu, B.; Lu, H.; Lu, Y. Study on the Treatment of Ammonia-nitrogen Wastewater. *Leather Manuf. Environ. Technol.* **2022**, *3*, 19–21.
10. Fu, R.; Zhang, P.-S.; Jiang, Y.-X.; Sun, L.; Sun, X.-H. Wastewater treatment by anodic oxidation in electrochemical advanced oxidation process: Advance in mechanism, direct and indirect oxidation detection methods. *Chemosphere* **2023**, *311*, 136993. [CrossRef]
11. Yu, H.; Li, Y.; Zhao, M.; Dong, H.; Yu, H.; Zhan, S.; Zhang, L. Energy-saving removal of methyl orange in high salinity wastewater by electrochemical oxidation via a novel Ti/SnO_2-Sb anode-air diffusion cathode system. *Catal. Today* **2015**, *258*, 156–161. [CrossRef]
12. Shi, H.; Gao, M.; Xu, Z.; Ma, Z.; Ni, J.; Xu, Y.; Wang, Q. Long-term performance of granular activated carbon electrode system for the removal of amoxicillin. *J. Water Process. Eng.* **2022**, *46*, 102397. [CrossRef]

13. Guo, C.; Liu, H.; Wang, C.; Zhao, J.; Zhao, W.; Lu, N.; Qu, J.; Yuan, X.; Zhang, Y.-N. Electrochemical removal of levofloxacin using conductive graphene/polyurethane particle electrodes in a three-dimensional reactor. *Environ. Pollut.* **2020**, *260*, 114101. [CrossRef] [PubMed]
14. Ji, J.; Liu, Y.; Yang, X.-Y.; Xu, J.; Li, X.-Y. Multiple response optimization for high efficiency energy saving treatment of rhodamine B wastewater in a three-dimensional electrochemical reactor. *J. Environ. Manag.* **2018**, *218*, 300–308. [CrossRef] [PubMed]
15. Karthikeyan, S.; Viswanathan, K.; Boopathy, R.; Maharaja, P.; Sekaran, G. Three dimensional electro catalytic oxidation of aniline by boron doped mesoporous activated carbon. *J. Ind. Eng. Chem.* **2015**, *21*, 942–950. [CrossRef]
16. Wei, L.; Guo, S.; Yan, G.; Chen, C.; Jiang, X. Electrochemical pretreatment of heavy oil refinery wastewater using a three-dimensional electrode reactor. *Electrochim. Acta* **2010**, *55*, 8615–8620. [CrossRef]
17. Wang, B.; Shu, B.; Ren, H.; Wang, B. Effects of three dimensional electrode filling particles on treatment of MDEA effluent. *Chin. J. Environ. Eng.* **2017**, *11*, 205–210.
18. Zhong, R.; Zhou, D.; Chen, W.; Ji, Q. Investigation of the packing model of particle electrode on the efficiency of threedimensional electrode reactor. *Acta Sci. Circumstantiae* **2011**, *31*, 2174–2178.
19. Baddouh, A.; Bessegato, G.G.; Rguiti, M.M.; El Ibrahimi, B.; Bazzi, L.; Hilali, M.; Zanoni, M.V.B. Electrochemical decolorization of Rhodamine B dye: Influence of anode material, chloride concentration and current density. *J. Environ. Chem. Eng.* **2018**, *6*, 2041–2047. [CrossRef]
20. Sathishkumar, K.; AlSalhi, M.S.; Sanganyado, E.; Devanesan, S.; Arulprakash, A.; Rajasekar, A. Sequential electrochemical oxidation and bio-treatment of the azo dye congo red and textile effluent. *J. Photochem. Photobiol. B-Biol.* **2019**, *200*, 111655. [CrossRef]
21. Cui, X. Literature Review of DSA Electrode in Wastewater Treatment. *Environ. Dev.* **2011**, *23*, 58+63.
22. Iranpour, F.; Pourzamani, H.; Mengelizadeh, N.; Bahrami, P.; Mohammadi, H. Application of response surface methodology for optimization of reactive black 5 removal by three dimensional electro-Fenton process. *J. Environ. Chem. Eng.* **2018**, *6*, 3418–3435. [CrossRef]
23. Costa, C.R.; Botta, C.M.R.; Espindola, E.L.G.; Olivi, P. Electrochemical treatment of tannery wastewater using DSA® electrodes. *J. Hazard. Mater.* **2008**, *153*, 616–627. [CrossRef]
24. Kim, T.H.; Park, C.; Shin, E.B.; Kirm, S. Effects of Cl-based chemical coagulants on electrochemical oxidation of textile wastewater. *Desalination* **2003**, *155*, 59–65. [CrossRef]
25. Hu, B.; Wang, Y.; Hu, C.; Zhou, X. Design, fabrication and high efficient visible-light assisted photoelectric-synergistic performance of 3-D mesoporous DSA electrodes. *Mater. Des.* **2016**, *91*, 201–210. [CrossRef]
26. Wang, Y.; Hu, B.; Hu, C.; Zhou, X. Fabrication of a novel Ti/SnO_2-Sb-CeO_2@TiO_2-SnO_2 electrode and photoelectrocatalytic application in wastewater treatment. *Mater. Sci. Semicond. Process.* **2015**, *40*, 744–751. [CrossRef]
27. Tran Le, L. Post treatment of ICEAS-biologically landfill leachate using electrochemical oxidation with Ti/BDD and Ti/RuO_2 anodes. *Environ. Technol. Innov.* **2020**, *20*, 101099.
28. Chen, X.; Chen, G.; Gao, F.; Yue, P.L. High-performance Ti/BDD electrodes for pollutant oxidation. *Environ. Sci. Technol.* **2003**, *37*, 5021–5026. [CrossRef] [PubMed]
29. Vasilie, S.; Manea, F.; Baciu, A.; Pop, A. Dual use of boron-doped diamond electrode in antibiotics-containing water treatment and process control. *Process Saf. Environ. Prot.* **2018**, *117*, 446–453. [CrossRef]
30. Gao, C.; Chang, M. Ta/BDD Film Electrode for Electrochemical Oxidation Nitrophenol. *Acta Physico-Chim. Sin.* **2008**, *24*, 1988–1994.
31. Montilla, F.; Morallon, E.; Battisti, A.D.; Benedetti, A.; Vazquez, J.L. Preparation and Characterization of Antimony-Doped Tin Dioxide Electrodes. Part 2. XRD and EXAFS Characterization. *J. Phys. Chem.* **2004**, *108*, 5044–5050. [CrossRef]
32. Wang, B.Y.; Shi, Y.Q.; Liu, Z.Z.; Zhang, Y.C.; Wang, Y.L.; Lu, T.X.; Wan, S.-W.; Sun, X.-C. Research Progress of Electrode Materials for Electrochemical Water Treatment. *Environ. Sci. Technol.* **2022**, *45*, 197–207.
33. Perea, L.A.; Palma-Goyes, R.E.; Vazquez-Arenas, J.; Romero-Ibarra, I.; Ostos, C.; Torres-Palma, R.A. Efficient cephalexin degradation using active chlorine produced on ruthenium and iridium oxide anodes: Role of bath composition, analysis of degradation pathways and degradation extent. *Sci. Total Environ.* **2019**, *648*, 377–387. [CrossRef] [PubMed]
34. Ukundimana, Z.; Omwene, P.I.; Gengec, E.; Can, O.T.; Kobya, M. Electrooxidation as post treatment of ultrafiltration effluent in a landfill leachate MBR treatment plant: Effects of BDD, Pt and DSA anode types. *Electrochim. Acta* **2018**, *286*, 252–263. [CrossRef]
35. Oliveira, E.M.; Silva, F.R.; Morais, C.C.; Oliveira, T.M.B.; Martínez-Huitle, C.A.; Motheo, A.J.; Albuquerque, C.C.; Castro, S.S.L. Performance of (in)active anodic materials for the electrooxidation of phenolic wastewaters from cashew-nut processing industry. *Chemosphere* **2018**, *201*, 740–748. [CrossRef] [PubMed]
36. Zhu, X. Preparation of Titanium Based DSA Electrode and Performance and Mechanism of Electrochemical Oxidation of Aniline Wastewater. Ph.D. Thesis, China University of Geosciences (Peking), Beijing, China, 2020.
37. Yu, J.; Huang, S.; Li, Y.; Chen, Z. Treatment landfill leachate with three-dimensional electrodes coated by activated carbon. *Ind. Water Treat.* **2021**, *41*, 232–237.
38. Dai, H.; Chen, J.; Miao, X.; Jiang, B.; Gong, X. Effect of alcohols on scavenging efficiencies to hydroxyl radical in UV-Fenton system. *China Environ. Sci.* **2018**, *38*, 202–209.
39. Li, C.; Wang, H.; Cui, X. Treatment of cobalt and manganese containing wastewater by three-dimensional electrode method. *Environ. Prot. Chem. Ind.* **2021**, *41*, 43–48.

40. Jiang, H.; Zhou, D.; Chen, W.; Luo, B.; Fan, Z. Preliminary exploration of electrochemical reaction characteristics in three-dimensional electrode treatment ammonia waste water. *China Environ. Sci.* **2014**, *34*, 2551–2555.
41. Liang, H.; Zhao, L.; Li, L.; Chen, Y.; Peng, H. Catalytic oxidation of chlorine-containing hydroxypropyl guanidine gum simulated wastewater by three-dimensional electrode technology. *Ind. Water Treat.* **2020**, *40*, 40–44.
42. Li, N.; Wang, B.; Yuan, D. Progress on treatment of phenol-containing wastewater by electrochemical technology. *Mod. Chem. Ind.* **2021**, *41*, 33–37.
43. Chen, W.; Li, F.; Mei, P. Mechanism of COD Degradation in Wastewater Using Three Dimension Electrode Method. *Environ. Sci. Technol.* **2002**, *1*, 11–12+22–46. [CrossRef]
44. Wu, N.; Qian, H.; Zhen, L.; Li, Y.; Wang, Y.; Wang, L. Experimental Study on the Treatment of Malachite Green Dyeing Wastewater by Three-Dimensional Electrode Electro-Fenton Process. *J. Shenyang Jianzhu Univ. (Nat. Sci.)* **2018**, *34*, 183–192.
45. Li, Y.; Duan, Y. Treatment of Wastewater Containing High Concentration Ammonia-Nitrogen by Electrochemical Oxidation Process. *J. Adv. Mat. Res.* **2011**, *393–395*, 1587–1590. [CrossRef]
46. Li, Y.; Guo, P. Experiment on Treatment of Nitrobenzene Wastewater by Three-dimensional Electrode Electro-Fenton Method. *J. Shenyang Jianzhu Univ. (Nat. Sci.)* **2023**, *39*, 177–184.
47. Chen, L.; Zhu, J.; Li, J.; Ma, Z.; Yang, Y.; Wang, S. Electrochemical Treatment of DMF Wastewater by TiO_2/AC Three-dimensional Electrode. *Guangzhou Chem. Ind.* **2021**, *49*, 65–68.
48. Li, Y.; Xu, S.; Gao, C.; Fu, X. Treatment of reactive brilliant orange X-GN wastewater by three-dimensional electrode-electro-Fenton method. *Ind. Water Treat.* **2022**, *44*, 1–15. [CrossRef]
49. Yuan, J. Research status of ammonia wastewater treatment methods. *Sci. Technol. Vis.* **2020**, *21*, 160–161. [CrossRef]
50. Bu, J.; Deng, Z.; Liu, H.; Li, T.; Yang, Y.; Zhong, S. Bimetallic modified halloysite particle electrode enhanced electrocatalytic oxidation for the degradation of sulfanilamide. *J. Environ. Manag.* **2022**, *312*, 114975. [CrossRef]
51. Hou, Z.; Zhou, J.; Wu, L.; Liang, K.; Song, Y.; Zhang, Q. Study on Synergetic-Photoelectrocatalytic Degradation of Phenol by Nano-TiO_2 Three-dimensional Electrode. *Nonferrous Met. Eng.* **2019**, *9*, 1–6+28.
52. Zhang, L.; Duan, A.; Wang, L.; Fu, B.; Liu, X.; Wu, G. Advanced treatment of coking wastewater using three-dimensional fluid bed electrode reactor. *Ecol. Environ. Sci.* **2012**, *21*, 370–374.
53. Singla, J.; Verma, A.; Sangal, V.K. Applications of doped mixed metal oxide anode for the electro-oxidation treatment and mineralization of urine metabolite, uric acid. *J. Water Process Eng.* **2019**, *32*, 100944. [CrossRef]
54. Ozturk, D.; Yilmaz, A.E. Treatment of slaughterhouse wastewater with the electrochemical oxidation process: Role of operating parameters on treatment efficiency and energy consumption. *J. Water Process Eng.* **2019**, *31*, 100834. [CrossRef]
55. Ni, J. Study on the Effect of Loaded γ-MnO_2 Particales on the Degradation of Rhodamine B Wastewater by Three-Dimensional Electrode Reactor. Ph.D. Thesis, University of Science and Technology Beijing, Beijing, China, 2020.
56. Niu, X.; Xie, F. Preparation of Ti-base SnRuCo Electrode with Nano-coating. *Sci. Technol. Eng.* **2007**, *11*, 2564–2569+2598.
57. Wang, C.; Huang, Y.-K.; Zhao, Q.; Ji, M. Treatment of secondary effluent using a three-dimensional electrode system: COD removal, biotoxicity assessment, and disinfection effects. *Chem. Eng. J.* **2014**, *243*, 1–6.
58. Oliveira, K.S.G.C.; Farinos, R.M.; Veroli, A.B.L.; Ruotolo, A.M. Electrochemical incineration of glyphosate wastewater using three-dimensional electrode. *Environ. Technol.* **2021**, *42*, 170–181. [CrossRef]
59. Su, W.; Yang, J.; Cheng, Z.; Shi, J.; Xu, H. Improvement of a three-dimensional electrochemical reactor for styrene wastewater treatment. *Environ. Eng.* **2019**, *37*, 107–110.
60. Li, X. Development in electrochemical technology for environmental wastewater treatment. *Int. J. Electrochem. Sci.* **2022**, *17*, 2212110. [CrossRef]
61. Zhang, X.; Zhao, C.; Wang, D.; Zhao, Y.; Zhang, Y.; Guo, R. Electrocatalytic Performance of Three-dimensional Electrode System with SnO_2/Fe_3O_4 Particle Electrode. *Mater. Rep.* **2017**, *31*, 25–30.
62. Ding, W.; Li, Q.; Liang, G.; Xiang, X.; Zeng, X.; Su, Q. Characteristics of ammonia removal from water using biochar three-dimensional electrode reactor. *J. Harbin Inst. Technol.* **2016**, *48*, 131–135.

Disclaimer/Publisher's Note: The statements, opinions and data contained in all publications are solely those of the individual author(s) and contributor(s) and not of MDPI and/or the editor(s). MDPI and/or the editor(s) disclaim responsibility for any injury to people or property resulting from any ideas, methods, instructions or products referred to in the content.